Multiple-scattering solution to nonlinear mechanical properties of binary elastic-plastic composite media

Ce-Wen Nan and Run-Zhang Yuan
The National Laboratory of Advanced Technology of Materials Compositing, Wuhan University of Technology, Wuhan, Hubei 430070, China
(Received 15 September 1992; revised manuscript received 12 April 1993)

This paper is concerned with the description of the nonlinear mechanical properties of composite media. We develop a general theoretical framework for the determination of the overall nonlinear behavior of a two-phase composite, with randomly oriented elastic and ellipsoidal particles embedded in a ductile medium, in terms of the multiple-scattering theory. This theory is versatile enough to provide results under any proportionally increasing combined stress. Two solutions, namely, non-self-consistent and self-consistent solutions, for the nonlinear behavior are discussed. The theoretical predictions also compare reasonably with the experimental results.

I. INTRODUCTION

Many methods have been proposed to evaluate the linearly macroscopic behavior of heterogeneous media from constituent properties and interactions. Among the more prominent ones is the multiple-scattering theory,[1,2] which has been developed in various ways to describe the physical and mechanical properties of heterogeneous media in the linear-response regime.[3–6] Recently, the attention has shifted to the nonlinear response of these media because, in practice, there are many nonlinear behaviors.

Over the last few years, some work[7–11] on the nonlinear magnetic and dielectric susceptibilities of heterogeneous media has been reported. Recently, Ballabh *et al.*[12] have deduced the explicit analytical expression for the third-order elastic constant of disordered solids and calculated the three independent third-order elastic constants of cubic polycrystals by generalizing the multiple-scattering theory.

In this paper, we follow the multiple-scattering schemes and describe the strongly nonlinear mechanics behavior of a perfectly bonded elastic-plastic composite under a proportionally increasing (not cyclic) combined stress. In the limit of the low-volume concentration of elastic particles, our results reduce to those recently found by Tandon and Weng,[13] and Qui and Weng,[14] from an improved micromechanics model.

In Sec. II, we give the properties of the ductile phase and introduce the notations. In Sec. III, we present the general formulation which shows a latent correspondence principle between elasticity and elastoplasticity. Two kinds of approximate solutions, namely, non-self-consistent (NSC) and self-consistent (SC) solutions, of the overall nonlinear elastoplastic properties for the composite with spherical or spheroidal particles are given in Sec. IV. The results of the application of the theoretical methods to the ductile-matrix composites reinforced with hard particles are discussed in Sec. V, and Sec VI is devoted to the conclusions.

II. PRELIMINARIES

Since the theory is intended only for the monotonic and proportional loading, the deformation theory (instead of the incremental theory) will be used to describe the nonlinear stress-strain relation of the ductile phase. Under a uniaxial tension the nonlinear stress-plastic-strain relation of most ductile materials can usually be represented by the modified Ludwik equation.[13] In a composite system, the ductile phase is usually in a triaxial stress state and the Ludwik equation can be expressed as

$$\sigma^e=\sigma_y+h(\epsilon^{pe})^n , \tag{1}$$

in terms of von Mises' effective stress σ^e and strain ϵ^{pe}, defined by

$$\sigma^e=(3\sigma'_{ij}\sigma'_{ij}/2)^{1/2},\quad \epsilon^{pe}=(3\epsilon^p_{ij}\epsilon^p_{ij}/2)^{1/2} , \tag{2}$$

where σ'_{ij} is the deviatoric stress, ϵ^p_{ij} is the plastic strain, and σ_y, h, and n are the initial yield stress, strength coefficient, and work-hardening exponent, in turn.

The "secant" Young's modulus of the isotropic ductile phase is given by

$$E^s=1/\{1/E+\epsilon^{pe}/[\sigma_y+h(\epsilon^{pe})^n]\} , \tag{3}$$

where E is its ordinary linear Young's modulus. The assumption of plastic incompressibility for the ductile phase results in k^s (the secant bulk modulus)$=k$ (the linear elastic bulk modulus), and the secant shear modulus μ^s is given by

$$\mu^s=E^s/(3-E^s/3k) . \tag{4}$$

In the following analysis we use a general symbolic notation, that is, second-rank tensors are denoted by Greek letters; fourth-rank tensors are denoted by capital letters; and scalars are denoted by lower case, light-faced letters. All the tensors considered are dyadic ones, and the dot symbols in the inner products between tensors are ignored.

III. FORMALISM

Under a monotonically increasing proportional loading, the equations governing the mechanical response of the perfectly bonded elastic-plastic composite resemble, in their appearance forms, the linear elastic problem, namely,

$$\text{constitutive, } \sigma = C^s(\epsilon)\epsilon \ , \tag{5}$$

$$\text{equilibrium, } \nabla\cdot\sigma = 0 \ . \tag{6}$$

But in this case, these equations are nonlinear. Here σ denotes the stress tensor, ϵ the strain tensor, $C^s(\epsilon)$ the secant stiffness tensor which is a function of the strain field. These tensors are dependent on the spatial position r. The effective secant modulus C^{s*} of the composite can be defined in terms of averaged stress $\langle\sigma\rangle$ and strain $\langle\epsilon\rangle$, namely,

$$\langle\sigma\rangle = C^{s*}\langle\epsilon\rangle \ . \tag{7}$$

We introduce a modulus tensor C_0^s which depends on the homogeneous strain field ϵ^0 in a homogeneous reference medium. In the case of the homogeneous boundary conditions of a uniform applied field, C_0^s does not have a spatial variations. The secant modulus tensor $C^s(\epsilon)$ is now

$$C^s(\epsilon) = C_0^s + \delta C^s(\epsilon) \ , \tag{8}$$

where $\delta C^s(\epsilon)$ is the fluctuation on C_0^s.

Under a prescribed surface displacement, the strain field within the composite can be obtained as

$$\epsilon = \epsilon^0 + G\delta C^s(\epsilon)\epsilon \ , \tag{9}$$

where G is the familiar Green's-function tensor[1] for the homogeneous background medium C_0^s, which is given in the Appendix. Equation (9) has the iterative solution

$$\epsilon = \epsilon^0 + GT(\epsilon)\epsilon^0 \ , \tag{10}$$

with

$$\begin{aligned} T(\epsilon) &= \delta C^s(\epsilon) + \delta C^s(\epsilon)GT(\epsilon) \\ &= \delta C^s(\epsilon)[I - G\delta C^s(\epsilon)]^{-1} \\ &= \delta C^s + \delta C^s G\delta C^s + \delta C^s G\delta C^s G\delta C^s + \cdots \ , \end{aligned} \tag{11}$$

where I is the unit tensor. From these equations, we get the formal expression for the effective secant modulus C^{s*}:

$$C^{s*} = C_0^s + \langle T(\epsilon)\rangle\langle I + GT(\epsilon)\rangle^{-1} \ . \tag{12}$$

This expression is of the same form as the known equation used extensively for the determination of the effective linear-elastic modulus.[1,6] As mentioned above, Eqs. (5) and (6) are also of the same form as the corresponding elastic results if we identify $C^s(\epsilon)$ with the elastic modulus C. There then emerges a latent correspondence principle for nonlinearly elastoplastic properties of elastic-plastic composite media. It follows that the effective secant moduli of a binary elastic-plastic composite are obtained by simply replacing phase elastic moduli by the corresponding phase secant moduli in the expressions for the effective elastic moduli of an elastic composite with identical phase geometry. Similarly, we can obtain the same results under a prescribed traction (not presented here).

For a random composite, it is very difficult to calculate the total t matrix, Eq. (11), so the first approximation to $T(\epsilon)$ is usually taken as

$$T = \sum_n T^{(n)}, \quad T^{(n)} = \delta C^{s(n)} + \delta C^{s(n)} G T^{(n)} \ , \tag{13}$$

where the index (n) denotes particle n. There are generally two first-order approximations depending on the choice of C_0^s, namely, NSC ($C_0^s = C_1^s$, the secant modulus of the matrix phase) and SC ($C_0^s = C^{s*}$, effective-medium theory) approximations. The NSC approach gives the average stress in the matrix (phase 1) and the inclusions (phase 2), which is central to the determination of yield criterion, as

$$\sigma^{(1)} = C_1^s\langle(I + GT)C^{s*}\rangle^{-1}\langle\sigma\rangle \ , \tag{14a}$$

$$\sigma^{(2)} = C_2^s(I + GT^{(2)})\langle(I + GT)C^{s*}\rangle^{-1}\langle\sigma\rangle \ , \tag{14b}$$

and the SC approach gives

$$\begin{aligned} &\langle T\rangle = 0 \ , \\ &\sigma^{(i)} = C_i^s(I + GT^{(i)})\langle(I + GT)C^{s*}\rangle^{-1}\langle\sigma\rangle \ , \end{aligned} \tag{15}$$

where $\sigma^{(i)}$, C_i^s, and $T^{(i)}$ are the average stress, the modulus, and the t matrix of the ith phase, respectively.

IV. ANALYSIS

In order to have a better understanding of the results obtained in Sec. III, we consider a composite of two isotropic constituents. Let the inclusions (spheres or spheroids) be randomly distributed so that the composite is effectively isotropic and characterized by secant bulk and shear moduli k^{s*} and μ^{s*} to be found.

A. Spherical particles

For the composite with a ductile matrix (k_1,μ_1^s) and spherical inclusions (k_2,μ_2), we directly get the NSC results from Eq. (12):

$$\frac{k^{s*} - k_1}{3k^{s*} + 4\mu_1^s} = f_2\frac{k_2 - k_1}{3k_2 + 4\mu_1^s} \ , \tag{16a}$$

$$\frac{\mu^{s*} - \mu_1^s}{\mu^{s*} + y_1^s} = f_2\frac{\mu_2 - \mu_1^s}{\mu_2 + y_1^s} \ , \tag{16b}$$

where

$$y_1^s = y(k_1,\mu_1^s) = \frac{\mu_1^s(9k_1 + 8\mu_1^s)}{6(k_1 + 2\mu_1^s)} \ , \tag{16c}$$

and f_2 is the volume fraction of the inclusions. These NSC results are identical to those found by Tandon and Weng,[13] and Qiu and Weng[14] from an improved micromechanics theory, and are available for the case where the value of f_2 is small and the inclusions are completely

dispersed in the ductile matrix. By decomposing the stress into hydrostatic (σ_{kk}) and deviatoric (σ'_{ij}) parts, we get the average stress in the matrix

$$\sigma_{kk}^{(1)}=1/[1+4f_2\mu_1^s(k_2-k_1)/k_1(3k_2+4\mu_1^s)]\langle\sigma_{kk}\rangle\ , \tag{17a}$$

$$\sigma_{ij}'^{(1)}=1/[1+f_2y_1^s(\mu_2-\mu_1^s)/\mu_1^s(\mu_2+y_1^s)]\langle\sigma'_{ij}\rangle\ , \tag{17b}$$

from Eq. (14a). These results are also consistent with those derived in the literature.[13,14]

The SC results are obtained as

$$(1-f_2)\frac{k_1-k^{s*}}{3k_1+4\mu^{s*}}+f_2\frac{k_2-k^{s*}}{3k_2+4\mu^{s*}}=0\ , \tag{18a}$$

$$(1-f_2)\frac{\mu_1^s-\mu^{s*}}{\mu_1^s+y^{s*}}+f_2\frac{\mu_2-\mu^{s*}}{\mu_2+y^{s*}}=0\ , \tag{18b}$$

where $y^{s*}=y(k^{s*},\mu^{s*})$. In this case, the hydrostatic and deviatoric stresses in the ductile matrix are obtained as

$$\sigma_{kk}^{(1)}=[k_1(k_2-k^{s*})/(1-f_2)k^{s*}(k_2-k_1)]\langle\sigma_{kk}\rangle\ , \tag{19a}$$

$$\sigma_{ij}'^{(1)}=[\mu_1^s(\mu_2-\mu^{s*})/\mu^{s*}(1-f_2)(\mu_2-\mu_1^s)]\langle\sigma'_{ij}\rangle\ , \tag{19b}$$

from Eq. (15). Obviously, these SC results are different from the NSC results.

B. Randomly oriented spheroids

We now consider disklike and needle-shaped particles for convenience (in the Appendix, the Green's-function tensor is calculated for spheroidal-shaped particles). For disklike particles, the NSC results are obtained as

$$\frac{k^{s*}-k_1}{3k^{s*}+4\mu_2}=f_2\frac{k_2-k_1}{3k_2+4\mu_2}\ , \tag{20a}$$

$$\frac{\mu^{s*}-\mu_1^s}{\mu^{s*}+y_2}=f_2\frac{\mu_2-\mu_1^s}{\mu_2+y_2}\ , \tag{20b}$$

and

$$\sigma_{kk}^{(1)}=1/[1+4f_2\mu_2(k_2-k_1)/k_1(3k_2+4\mu_2)]\langle\sigma_{kk}\rangle\ , \tag{20c}$$

$$\sigma_{ij}'^{(1)}=1/[1+f_2y_2(\mu_2-\mu_1^s)/\mu_1^s(\mu_2+y_2)]\langle\sigma'_{ij}\rangle\ . \tag{20d}$$

These results are also similar to those recently derived by Qiu and Weng.[14] An interesting consequence of these results is that, in the case of disklike particles, the composite still remains plastically incompressible. Furthermore, the SC results are

$$(1-f_2)(k_1-k^{s*})\frac{3k^{s*}+4\mu_1^s}{3k_1+4\mu_1^s}+f_2(k_2-k^{s*})\frac{3k^{s*}+4\mu_2}{3k_2+4\mu_2}=0\ , \tag{21a}$$

$$(1-f_2)(\mu_1^s-\mu^{s*})\frac{\mu^{s*}+y_1^s}{\mu_1^s+y_1^s}+f_2(\mu_2-\mu^{s*})\frac{\mu^{s*}+y_2}{\mu_2+y_2}=0\ , \tag{21b}$$

and

$$\sigma_{kk}^{(1)}=[k_1(k_2-k^{s*})/(1-f_2)k^{s*}(k_2-k_1)]\langle\sigma_{kk}\rangle\ , \tag{21c}$$

$$\sigma_{ij}'^{(1)}=[\mu_1^s(\mu_2-\mu^{s*})/(1-f_2)\mu^{s*}(\mu_2-\mu_1^s)]\langle\sigma'_{ij}\rangle\ , \tag{21d}$$

Equations (21c) and (21d) are, in their appearance forms, the same as Eqs. (19a) and (19b), respectively.

For needle-shaped particles, the NSC results are

$$\frac{k^{s*}-k_1}{3k^{s*}+3\mu_1^s+\mu_2}=f_2\frac{k_2-k_1}{3k_2+3\mu_1^s+\mu_2}\ , \tag{22a}$$

$$\frac{\mu^{s*}-\mu_1^s}{\mu^{s*}+z^s}=f_2\frac{\mu_2-\mu_1^s}{\mu_2+z^s}\ , \tag{22b}$$

where

$$z^s=z(\mu_1^s,\mu_2,w^s)=\frac{\mu_2w^s-\mu_1^s}{1-w^s}\ ,$$

$$w^s=w(k_1,\mu_1^s;k_2,\mu_2)=\frac{1}{5}\left[\frac{4\mu_1^s(3k_1+4\mu_1^s)}{\mu_2(3k_1+4\mu_1^s)+\mu_1^s(3k_1+3\mu_2+\mu_1^s)}+\frac{3k_2+4\mu_1^s}{3k_2+3\mu_1^s+\mu_2}+\frac{4\mu_1^s}{\mu_2+\mu_1^s}\right]\ ,$$

and

$$\sigma_{kk}^{(1)}=1/[1+f_2(\mu_2+3\mu_1^s)\times(k_2-k_1)/k_1(3k_2+\mu_2+3\mu_1^s)]\langle\sigma_{kk}\rangle\ , \tag{22c}$$

$$\sigma_{ij}'^{(1)}=1/[1+f_2z^s(\mu_2-\mu_1^s)/\mu_1^s(\mu_2+z^s)]\langle\sigma'_{ij}\rangle\ . \tag{22d}$$

These NSC results are similar to those derived by Qiu and Weng.[14] Furthermore, the SC results are

$$(1-f_2)(k_1-k^{s*})\frac{3k^{s*}+3\mu^{s*}+\mu_1^s}{3k_1+3\mu^{s*}+\mu_1^s}+f_2(k_2-k^{s*})\frac{3k^{s*}+3\mu^{s*}+\mu_2}{3k_2+3\mu^{s*}+\mu_2}=0\ , \tag{23a}$$

$$(1-f_2)(\mu_1^s-\mu^{s*})\frac{\mu^{s*}+z_1^s}{\mu_1^s+z_1^s}+f_2(\mu_2-\mu^{s*})\frac{\mu^{s*}+z_2^s}{\mu_2+z_2^s}=0\ , \tag{23b}$$

where

$$z_1^s=z(\mu^{s*},\mu_1^s,w_1^s),\quad w_1^s=w(k^{s*},\mu^{s*};k_1,\mu_1^s)\ ,$$

$$z_2^s=z(\mu^{s*},\mu_2,w_2^s),\quad w_2^s=w(k^{s*},\mu^{s*};k_2,\mu_2)\ ,$$

and

$$\sigma_{kk}^{(1)}=[k_1(k_2-k^{s*})/(1-f_2)k^{s*}(k_2-k_1)]\langle\sigma_{kk}\rangle\ , \tag{23c}$$

$$\sigma_{ij}'^{(1)}=[\mu_1^s(\mu_2-\mu^{s*})/(1-f_2)\mu^{s*}(\mu_2-\mu_1^s)]\langle\sigma_{ij}'\rangle\ . \tag{23d}$$

Equations (23c) and (23d) also resemble, in their appearance forms, Eqs. (19a) and (19b).

V. NUMERICAL RESULTS AND APPLICATION

As an application of the above-theoretical solutions, we have calculated the overall nonlinear stress-strain properties of the silicon-carbide/6061-aluminum composite which is of great practical importance. The elastic and plastic properties of both phase are, $k_1=66.96$ GPa, $\mu_1=25.68$ GPa, $\sigma_y^{(1)}=250$ MPa, $h=173$ MPa, and $n=0.455$ for the aluminum matrix, $k_2=247.5$ GPa and $\mu_2=209.4$ GPa for SiC particles.[15] The obtained results are depicted in Figs. 1–5.

At low concentrations of SiC particles, NSC results are nearly identical to SC results. The wide difference between them occurs with the increase in the volume fraction. The reason for the wide difference is not difficult to understand. The interactions among the particles are taken into account by a mean field in a SC solution, and are ignored in a NSC solution. A SC solution is an improvement over a NSC solution. Figure 5 shows the favorable comparison between theoretical results and experimental data[15] for the same composite system with randomly oriented platelets ($f_2=0.2$, $r=0.25$). In this case, the NSC solution underestimates the flow stress in the plastic range, and the SC solution overestimates the flow stress only in the larger plastic strain. For the initial yield strength, the NSC solution only predicts a simply linear volume-fraction dependence (Fig. 4).

The shape of particles is seen to have a pronounced effect on the overall response (Figs. 1–4). As in the linear-elastic case, the oblate spheroids provide the most effective reinforcement and the spheres are the least effective, with the prolate spheroids lying between the two. The overall nonlinear behavior (plastic behavior) of the composite is more sensitive to the particle shape than the linear-elastic behavior. The shape and the volume fraction of particles are two important parameters which have a drastic effect on the nonlinear behavior of the composite.

VI. CONCLUSION

In this work we have developed a relatively simple multiaxial theory of a strongly nonlinear mechanical property (plasticity), which allows one to determine the

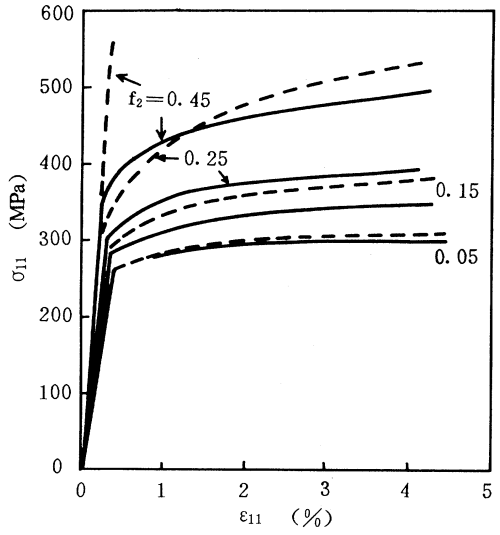

FIG. 1. Nonlinear stress-strain curves of aluminum-matrix composite reinforced with spherical silicon-carbide particles. The solid and dashed lines denote NSC and SC results, respectively.

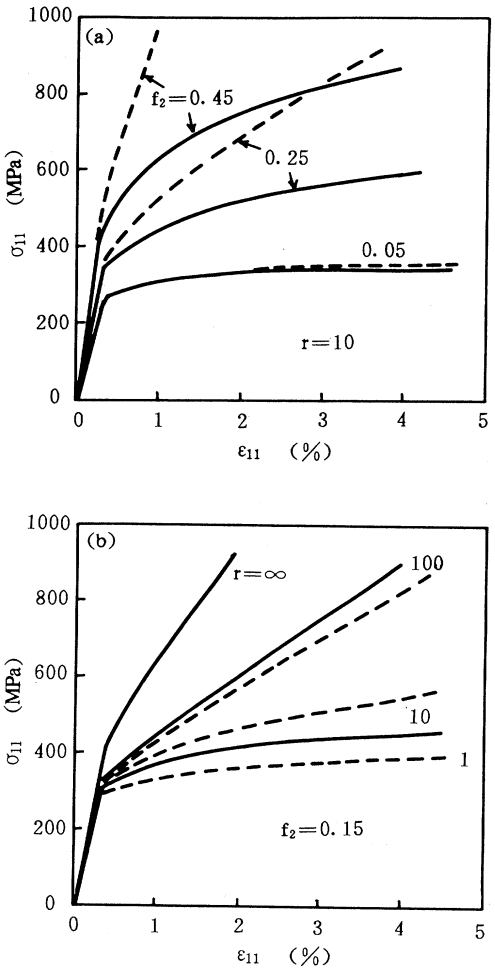

FIG. 2. The effect of (a) the volume fraction f_2 and (b) the aspect ratio r, of the prolate SiC particles on the nonlinear stress-strain curves of SiC-aluminum composites. The solid and dashed lines denote NSC and SC results, respectively.

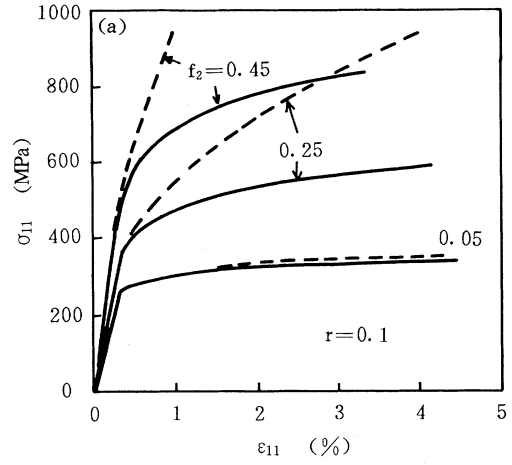

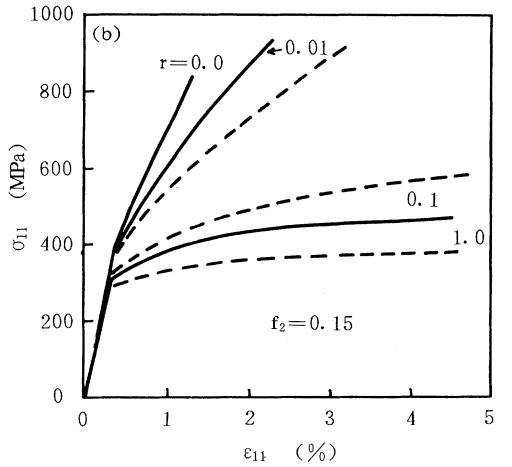

FIG. 3. The effect of (a) the volume fraction f_2 and (b) the aspect ratio r, of the oblate SiC particles on the nonlinear stress-strain curves of SiC-aluminum composites. The solid and dashed lines denote NSC and SC results, respectively.

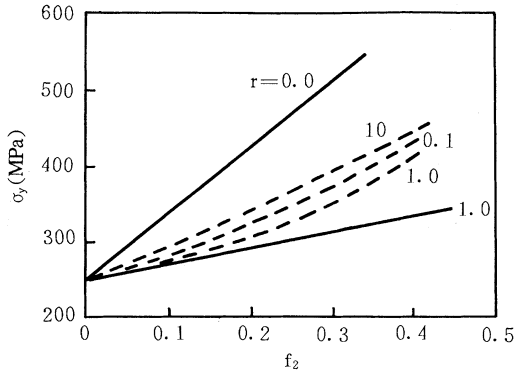

FIG. 4. The initial yield strength of the composites vs the volume fraction of SiC particles with different aspect ratios. The solid and dashed lines denote NSC and SC results, respectively.

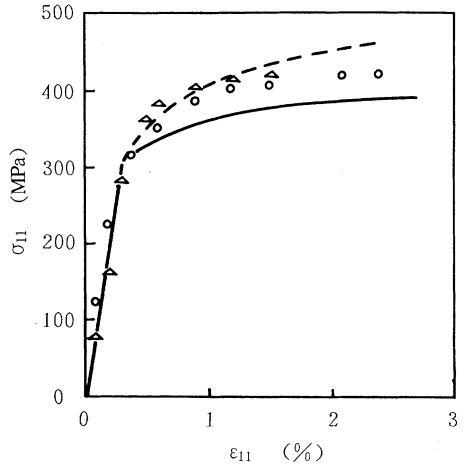

FIG. 5. Comparison between the theoretical predictions (solid line, NSC; dashed line, SC result) and the experimental data (Ref. 15) (open triangles, 0% reduction and T6 heating; open circles, 10% reduction and T6 heating) of a SiC-Al composite, with platelet-type reinforcement at $r=0.25$ and $f_2=0.2$.

overall nonlinear stress-strain relations of a two-phase, isotropic composite with spheroidal particles embedded in a medium. For the SiC-Al composite, explicit numerical calculations have been done following two different methods of solutions, namely, the NSC and SC approaches. The shape of the particles have a more dramatic effect on the nonlinear behavior than the linear one. It may be mentioned that NSC and SC solutions are believed to be the most reasonable approaches in the low concentration range. At high concentrations, there are several new problems which need to be addressed. The position of the particles will be correlated and the interactions among the particles need to be included. The fields outside the ellipsoidal particles are concentrated at the tips and can lead to decrease in the host medium flow stress.

ACKNOWLEDGMENTS

This work was supported by the National H-Tech Program under Contract No. 863-7152101. Thanks are due to Professor Fu-sheng Jin and Dr. Qing-jin Zhang for helpful discussions.

APPENDIX: GREEN'S-FUNCTION TENSOR

For an ellipsoid ($a=b\neq c$) with the symmetric axis identified as x_1, the components of the Green's-function tensor G_{ijkl} are

$$
\begin{aligned}
&G_{1111}=-3h(1-L_1)-g(L_1+L_2)/2\ ,\\
&G_{1122}=G_{1133}=G_{2211}=G_{3311}=g(L_1+L_2)/4\ ,\\
&G_{2222}=G_{3333}=-g(5L_1+3L_2)/16-3hL_1/2\ ,\\
&G_{2233}=G_{3322}=g(L_1-L_2)/16\ ,\\
&G_{1212}=G_{1313}=g(3L_1+2L_2-2)/8-3h(2-L_1)/8\ ,\\
&G_{2323}=-g(3L_1+L_2)/16-3hL_1/4\ ,
\end{aligned}
\tag{A1}
$$

where

$$g=(3k_0^s+\mu_0^s)/\mu_0^s(3k_0^s+4\mu_0^s),\quad h=1/(3k_0^s+4\mu_0^s)\ , \tag{A2}$$

$$L_1=r^2/(r^2-1)-r(r^2-1)^{-3/2}\cosh^{-1}r\ ,$$

for prolate spheroids , (A3)

$$L_1=r^2/(r^2-1)+r(1-r^2)^{-3/2}\cos^{-1}r\ ,$$

for oblate spheroids , (A4)

$$L_2=r^2(2-3L_1)/(r^2-1)\ , \tag{A5}$$

$$r=c/a\ . \tag{A6}$$

For a sphere, they reduce to

$$\begin{aligned} &G_{1111}=G_{2222}=G_{3333}=-h-2g/15\ ,\\ &G_{1122}=G_{1133}=G_{2211}=G_{3311}=G_{2233}=G_{3322}=g/15\ ,\\ &G_{1212}=G_{2323}=G_{1313}=-g/10-h/2\ . \end{aligned} \tag{A7}$$

For a needle with $r\to\infty$, the only nonvanishing components are

$$\begin{aligned} &G_{2222}=G_{3333}=-g/8-3h/2\ ,\\ &G_{2233}=G_{3322}=g/8\ ,\\ &G_{1212}=G_{1313}=-g/8-3h/8\ ,\\ &G_{2323}=-g/8-3h/4\ . \end{aligned} \tag{A8}$$

For a thin disc with $r\to 0$, the components are

$$\begin{aligned} &G_{1111}=-3h\ ,\\ &G_{1212}=G_{1313}=-(g+3h)/4\ , \end{aligned} \tag{A9}$$

and all other components are zero.

[1]R. Zeller and P. H. Dederichs, Phys. Status Solidi B **55**, 831 (1973).
[2]J. E. Gubernatis and J. A. Krumhansl, J. Appl. Phys. **46**, 1875 (1975).
[3]M. Hori and F. Yonezawa, J. Phys. C **10**, 229 (1977).
[4]M. Gomez, L. Fonseca, G. Rodriguez, A. Velazquez, and L. Gruz, Phys. Rev. B **32**, 3429 (1985).
[5]T. R. Middya and A. N. Basu, J. Appl. Phys. **59**, 2368 (1986).
[6]C. W. Nan, Prog. Mater. Sci. **37**, 1 (1993).
[7]G. S. Agarwal and S. D. Gupta, Phys. Rev. A **38**, 5678 (1988).
[8]D. Stroud and P. M. Hui, Phys. Rev. B **37**, 8719 (1988).
[9]J. W. Haus, N. Kalyaniwalla, R. Inguva, and C. M. Bowden, J. Opt. Soc. Am. B **6**, 797 (1989).
[10]J. W. Haus, R. Inguva, and C. M. Bowden, Phys. Rev. A **40**, 5729 (1989).
[11]N. C. Kothari, Phys. Rev. A **41**, 4486 (1990).
[12]T. K. Ballabh, M. Paul, T. R. Middya, and A. N. Basu, Phys. Rev. B **45**, 2761 (1992).
[13]G. P. Tandon and G. J. Weng, J. Appl. Mech. **55**, 126 (1988).
[14]Y. P. Qiu and G. J. Weng, Int. J. Solids Struct. **12**, 1537 (1991).
[15]R. J. Arsenault, Mater. Sci. Eng. **64**, 171 (1984).